

Journal of the Brazilian Chemical Society



This is an Open Access article distributed under the terms of the Creative Commons Attribution License, which permits unrestricted use, distribution, and reproduction in any medium, provided the original work is properly cited. Fonte: http://www.scielo.br/scielo.php?script=sci_arttext&pid=S0103-50532017000701288&lng=en&nrm=iso. Acesso em: 7 fev. 2018.

REFERÊNCIA

NEVES, Diana B. J. et al. Detection of counterfeit Durateston using Fourier transform infrared spectroscopy and partial least squares: discriminant analysis. **Journal of the Brazilian Chemical Society**, São Paulo, v. 28, n. 7, p. 1288-1296, jul. 2017. Disponível em: <http://www.scielo.br/scielo.php?script=sci_arttext&pid=S0103-50532017000701288&lng=en&nrm=iso>. Acesso em: 7 fev. 2018. doi: <http://dx.doi.org/10.21577/0103-5053.20160293>.



Detection of Counterfeit Durateston® Using Fourier Transform Infrared Spectroscopy and Partial Least Squares - Discriminant Analysis

Diana B. J. Neves,^a Márcio Talhavini,^a Jez Willian B. Braga,^b Jorge J. Zacca^a and Eloisa D. Caldas^{*c}

^aInstituto Nacional de Criminalística, Polícia Federal, 70610-200 Brasília-DF, Brazil

^bInstituto de Química and ^cLaboratório de Toxicologia, Departamento de Farmácia, Universidade de Brasília, 70910-900 Brasília-DF, Brazil

Medicines containing anabolic steroids are one of the main targets for counterfeiting worldwide, including Brazil. The aim of this work was to propose a method for discriminating original and counterfeit Durateston® ampoules by Fourier transform infrared spectroscopy (FTIR) followed by chemometric analysis. Ninety-six ampoules of Durateston®, 49 originals and 47 counterfeits, were analyzed by gas chromatography with mass spectrometry (GC-MS) and by FTIR. Principal component analysis was applied to the infrared spectra to detect different clusters, corresponding to original samples and different types of counterfeits. A partial least squares - discriminant analysis method was proposed to discriminate original samples from those counterfeits that were indistinguishable from the originals in the infrared analysis. A training subset comprised of one-third of the available spectra was used to establish a suitable model that correctly discriminated all samples in the test subset, resulting in 0% of false positive or negative results and 100% of efficiency rate, sensitivity and specificity. In addition to the low cost of the infrared technique, the proposed method is fast, reliable and suitable to replace GC-MS methods used in Durateston® ampoule analyses to detect counterfeiting.

Keywords: medicine counterfeiting, Durateston, FTIR, PCA, PLS-DA

Introduction

According to the World Health Organization (WHO), spurious/falsely-labeled/falsified/counterfeit medicines are those deliberately and fraudulently mislabeled with respect to their identity and/or source.¹ Counterfeit medicines pose a significant health risk to their consumers, as they can cause treatment failure, toxic reactions, and even death.^{2,3} It is not possible to ascertain the actual incidence of counterfeiting worldwide and the only data available are estimates. These range from less than 1% of the medicine market in some developed countries with well-established control policies, to 30% in developing countries in Africa, Asia and some regions of Latin America.²⁻⁴ Up to 50% of medicines sold on the internet are counterfeit, mostly from companies with no declared physical address.^{2,3,5}

Counterfeit medicines may include products with the correct active pharmaceutical ingredients (API) but at

concentrations different from those stated on the label, with incorrect API, no API, or only a mixture of toxic substances.^{2,3} All therapeutic classes are potential targets for counterfeiting, and the most common worldwide are antibiotics, hormones and steroids, antihistaminics, antimalarials, analgesics, and those in the genitourinary and central nervous system therapeutic categories.^{2,3} A study conducted with data obtained from forensic reports issued by the Brazilian Federal Police (BFP) from 2007 to 2010 showed that the main seized counterfeit medicines of declared national origin were those for erectile dysfunction (69%) and anabolic steroids (26%).⁶ Among the anabolic steroids, the most frequent was Durateston®, a Brazilian medicine currently manufactured by Aspen Pharma that accounted for 8.9% of all seizures and was the third most frequent counterfeit medicine overall (behind Viagra® and Cialis® only).⁶ A study conducted by our research group (not published) found that 11.9% of the 25,833 medicines of different origins seized by the BFP from 2006 to 2012 were anabolic steroids, the second most prevalent class after medicines for erectile dysfunction. Approximately

*e-mail: eloisa@unb.br

10% of all medicines were counterfeits, with Durateston® the third most frequent.

Another study showed that 31.7% of the 3,537 medicines seized by the BFP between 2006 and 2011 that declared to contain anabolic steroids were counterfeits, with 48.6% not containing any API and 28.3% containing APIs different from those stated on their labels.⁷ The second most seized medicine of this dataset was Durateston® (N = 264), of which 69.7% were counterfeits (89 had no API and 57 had only some of the four testosterone esters they should contain) (unpublished results).

Even though anabolic steroids are an important target for medicine counterfeiting, there are not many studies reporting the analysis of suspected medicines of this class. Those available relied mainly on gas or liquid chromatography analysis.⁸⁻¹² Spectroscopic techniques such as Raman, near infrared, and Fourier transform infrared (FTIR), together with chemometric tools, are being successfully used to analyze suspected counterfeit medicines.¹³⁻¹⁹ They have the advantage of being less time-consuming than chromatographic methods, with little or no sample preparation.^{13-15,19} However, to the best of our knowledge, only one work using spectroscopic methods to analyze anabolic steroid medicines has been published so far, describing the investigation of the composition of methandrostrenolone-containing tablets by near infrared and Raman spectroscopy.²⁰

The aim of this work was to develop a simple, fast, low-cost and reliable method for the detection of Durateston® counterfeits using FTIR and partial least squares - discriminant analysis (PLS-DA).

Experimental

Samples

A total of 96 ampoules of Durateston® were analyzed at the National Institute of Criminalistics (NIC) of the BFP in Brasilia, Federal District. Seventy-six ampoules were seized between 2009 to 2013 by the BFP in different regions of Brazil, mainly Foz do Iguacu and other cities on the Parana State (border with Paraguay), 29 of which were originals and 47 counterfeits. After being seized, the samples were stored at room temperature, and analyzed within the expiring date reported in the label. In order to account for batch-to-batch variability, 20 additional original ampoules from 8 different batch numbers were purchased at local pharmacies in Brasilia in March 2014, adding up to 49 original ampoules.

Fourier transform infrared

An IS10 FTIR Spectrometer (Nicolet Instrument Corp.,

Madison, USA) equipped with a DTGS detector (at room temperature) and an ATR (attenuated total reflectance) accessory with a single bounce diamond crystal was used for all experiments. Measurements were made with a single droplet of the ampoule content deposited directly on the ATR crystal, with no pressure applied to the droplet. Each spectrum consisted of 16 co-added scans measured at a resolution of 4 cm⁻¹ in the 4000-650 cm⁻¹ range. Spectra were collected and analyzed with OMNIC software, version 5.2.

After each measurement, the diamond crystal surface was cleaned with ethanol and dried. A spectrum preview was performed before adding a new sample to the diamond surface to ensure complete removal of the previous sample and the ethanol. Each spectrum yielded 6,949 variables (wavelengths).

Gas chromatography coupled with mass spectrometry (GC-MS)

All Durateston® ampoules were analyzed by GC-MS as a reference method, using a NIC screening method for forensic analysis of medicines and drugs. Analyses were qualitative and performed using a GC 6890N coupled with a MS 5973 Inert (Agilent Technologies, Palo Alto, CA, USA), with either Rxi-1MS (Restek Corporation, Bellefonte, PA, USA) or HP5-MS columns (Agilent Technologies). Samples were prepared by adding approximately five droplets of the sample to 1.0 mL of chloroform or methanol directly in a vial, which was homogenized and injected in the GC without further preparation. Results were analyzed with Enhanced MSD ChemStation D.02.00.275 (Agilent Technologies) and NIST MS Search 2.0 (distributed by Agilent Technologies).

Chemometrics

All data processing and modeling were performed using the Unscrambler X, v. 10.1 software (Camo software, Oslo).

Principal component analysis (PCA)

Principal component analysis (PCA) may be used as a first stage of chemometric processing, being applied as an exploratory data analysis tool, and for outlier detection.^{13,15,17} It reduces the number of variables by making linear orthogonal combinations of the original variables, called the principal components (PCs), which progressively explain the remaining variability in the data.^{13,15}

In this study, PCA was performed with all available spectra for exploratory analysis. Preprocessing included

baseline offset correction, first derivative smoothing (Savitzky-Golay, fourth order polynomial, 5 smoothing points) and data mean centering. The NIPALS algorithm was used for the principal components computation. A first PCA was performed using all variables in order to evaluate its loadings plot. Two spectral ranges (from 4000 to 3687 cm^{-1} , and from 2716 to 1810 cm^{-1}) could be excluded due to their insignificant influence (loadings values around zero) to explain the variance. A new PCA was then performed with the remaining variables and a full cross validation.

Partial least squares - discriminant analysis (PLS-DA)

Despite the discriminating tendencies that may be observed in the score plot, PCA cannot be used alone for classification or discrimination problems, for which supervised models such as partial least squares - discriminant analysis (PLS-DA) or soft independent modelling of class analogies (SIMCA) are more appropriated.^{17,20} PLS-DA is also based on the PCA decomposition, the difference being that the combinations of variables, called PLS factors or latent variables, are defined in such a way that the covariance of the instrumental data with the response variable (predefined classes) are maximized, leading to quantitative methods with low errors and high discrimination power between the different classes in discriminant analysis.^{13,15,18,20}

PLS-DA is performed using binary coding, in which a dummy discrete response vector y is attributed to the data set, such as 0 for counterfeit samples and 1 for original samples.^{14,17,21,22} In the training stage, the method is trained to assign "membership values", one for each class; a test sample is then assigned to a specific class if its y value surpasses a specific prediction threshold that may be estimated by establishing confidence limits for each sample classified.^{17,21,23} Therefore, estimated values in y are approximations of 0 or 1, and a good discrimination is obtained when the distributions of the estimated values belonging to classes 1 and 0 are not overlapped.²²

In this study, PLS-DA was applied using the same spectral regions and pre-processing methods as with PCA. The number of latent variables for the model was defined using the smallest root mean squared error of cross-validation (RMSECV) determined by full cross-validation (leave-one-out approach) in the training set. The outlier identification was performed based on the Hotelling T^2 and residuals Q , both considering the confidence level of 95%.²³ The discrimination threshold for each class was defined as 0.5, and a confidence interval of 95% was estimated for each test sample. Validation was performed by an independent test set comprised of a significant part of

all samples available for this study and the figures of merit false positive and negative rates, specificity, sensitivity and efficiency rate estimated according to Botelho *et al.*²⁴

Results and Discussion

Sample composition

All ampoules were analyzed by FTIR and GC-MS as previously described. Some examples of counterfeit Durateston® seized by the BFP are shown in Figure 1. The declared Durateston® composition, found in the original products (OR), is testosterone propionate, decanoate, phenpropionate and isocaproate (Figure 2), with benzyl alcohol and peanut oil as excipients. The chemical analysis obtained for the OR products (four esters identified by GC-MS analysis, and the vegetable oils by FTIR) matched this formulation.

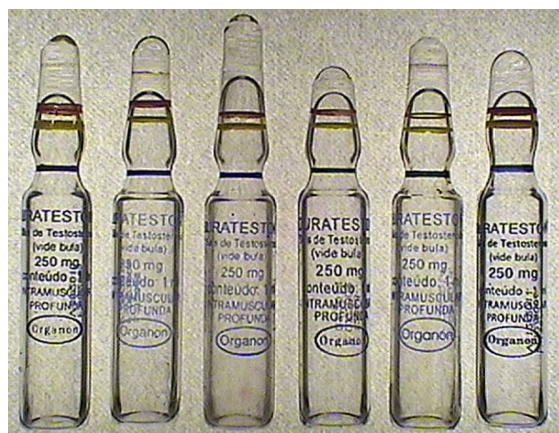


Figure 1. Different ampoules of counterfeit Durateston® compared with an original ampoule (far left). Picture taken with transmitted light.

Three different counterfeit types were identified in the samples: those containing only the excipient benzyl benzoate (BB), those containing testosterone propionate and prasterone (TP-PR), and those containing only testosterone propionate (TP). A total of 178 spectra of the ampoules were obtained: 93 from original samples and 85 from counterfeits (Table 1).

Chemical analysis for the BB category showed a single peak in the GC-MS chromatogram corresponding to benzyl benzoate, and a match for benzyl benzoate in the FTIR. The ampoules classified as TP-PR showed two peaks in the GC-MS, corresponding to testosterone propionate and prasterone (another steroidal hormone), and a match for propylene glycol in the FTIR. The TP was the most diverse category, with chromatograms of some samples showing one peak corresponding to testosterone propionate, and three or four others that yielded varying matches for

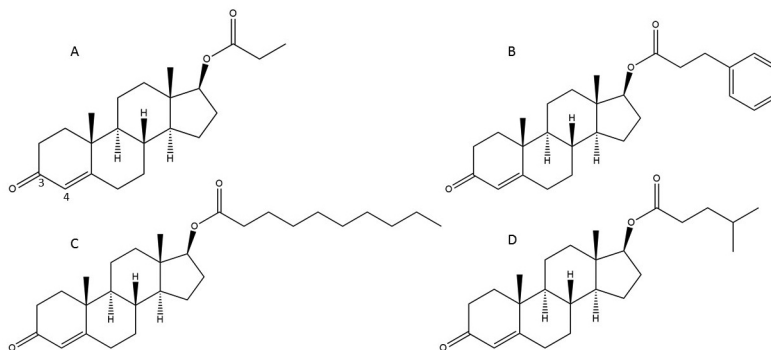


Figure 2. Testosterone esters: (A) propionate; (B) phenpropionate; (C) decanoate and (D) isocaproate. Numbers on (A) indicate the relevant carbons for FTIR spectra (Figure 3A).

Table 1. Number of ampoules and spectra and summary of the analysis results of the 96 Durateston® ampoules analyzed

Category	Number of ampoules and spectra	GC-MS and FTIR results
Original	49 ampoules (27 with one spectrum each; 22 with three spectra each), total of 93 spectra	contain the testosterone esters propionate, decanoate, phenpropionate and isocaproate, main excipient is a vegetable oil
BB	28 ampoules (16 with one spectrum each; 12 with three spectra each), total of 52 spectra	contain only benzyl benzoate, no API
TP-PR	1 ampoule with 3 spectra	contain testosterone propionate and prasterone, main excipient is propylene glycol
TP	18 ampoules (12 with one spectrum each; 6 with three spectra each), total of 30 spectra	contain testosterone propionate and no other API, main excipient is either a vegetable oil, an ester (such as allyl octanoate) or propylene glycol

OR: original product; TP: only testosterone propionate; TP-PR: testosterone propionate and prasterone; BB: only the incipient benzyl benzoate; API: active pharmaceutical ingredient.

different long-chain esters, such as allyl octanoate or allyl decanoate. Three ampoules in this category presented chromatograms that only exhibited the testosterone propionate peak. FTIR results of ampoules from the TP category were also dissimilar: samples not presenting the ester peaks had a match for propylene glycol, whereas the others had good matches for vegetable oils and for esters (allyl octanoate or methyl decanoate, whose spectra are very similar). Representative chromatograms of all categories are shown on Supplementary Information (SI, Figures S1 to S4).

Representative FTIR spectra of the four categories are shown in Figure 3. Spectra shown in Figure 3A (OR ampoules) and 3B (TP ampoules) are similar, given that

the vegetable oils present in OR ampoules and in some TP, and the long chain esters present in TP have similar spectra. One difference between these spectra is the presence of a narrow band of 1677 cm^{-1} , indicated by the arrow in Figure 3A, which is characteristic of 4-en, 3-one steroids, such as testosterone (Figure 2).²⁵ This band, however, is not significant enough to be discriminated by the FTIR library search, which gave similar results for the spectra shown in Figures 3A and 3B. The large, narrow band at around 1740 cm^{-1} , present in both the OR and TP spectra, is common to esters, and suffers mild dislocations according to the substituent group.^{26,27} The benzyl benzoate spectrum in Figure 3C stands out in relation to the others, mainly due to a band at around $720\text{--}680\text{ cm}^{-1}$ that refers to aromatic C–H bonds.^{26,27} The propylene glycol spectrum displayed in Figure 3D is the most distinguishable of the group, mainly due to the large –OH band at around 3300 cm^{-1} .²⁷

PCA

The PCA results for all the 178 spectra, after the exclusion of the two spectral regions ($4000\text{--}3687\text{ cm}^{-1}$ and $2716\text{--}1810\text{ cm}^{-1}$; Principal component analysis (PCA) section) are shown by the score plots of $\text{PC1} \times \text{PC2}$ (Figure 4A) and $\text{PC1} \times \text{PC2} \times \text{PC3}$ (Figure 4B). No samples with simultaneous high leverage and high residual variance (outliers) were detected. The first two PCs describe 92% of the data variation, and allow a clear distinction to be made of three groups, based on their excipients. Group 1 is comprised only of BB ampoules, group 2 of the TP-PR ampoules (whose excipient was propylene glycol) and TP ampoules which also contain propylene glycol, and group 3 containing the OR and the remaining TP ampoules (Figure 4A). By using 3 PCs (Figure 4B), it was possible to explain 97% of the total variance, and to fully separate the OR from the TP in group 3, although each was split into two subgroups. It was not possible, however, to separate TP-PR from those TP ampoules that contained propylene

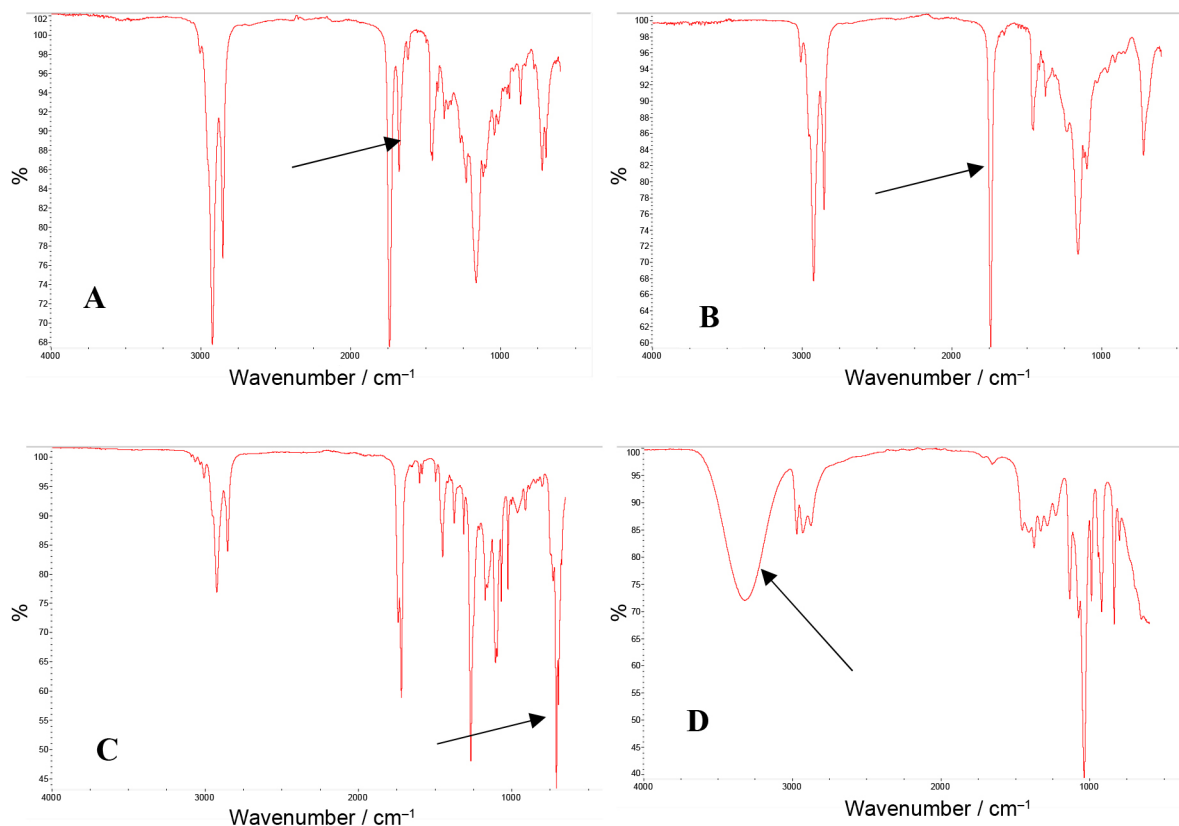


Figure 3. Representative FTIR spectra of seized Durateston® ampoules. (A) OR (good matches for several vegetable oils); (B) TP (good matches for vegetable oils and esters); (C) BB (good match for benzyl benzoate and furfuryl benzoate); (D) TP-PR (match for propylene glycol). The arrow on (A) indicates the band characteristic of 4-en, 3-one steroids; arrow on (B) indicates the band characteristic of esters; arrow on (C) indicates the band characteristic of C–H aromatic bonds and the arrow on (D) the band characteristic of –OH groups.

glycol in group 2 (Table 1). Loadings plots for the three PCs are displayed as Supplementary Information. These plots highlight that PC1 is responsible for separating BB ampoules from the rest (high loadings values at the 700 cm^{-1} region, corresponding to the strong band of aromatic C–H bonds as shown in Figure 3C) (SI, Figure S5). PC2 is responsible for separating samples containing propylene glycol from those with vegetable oils; its loading plots show several relevant regions around 2900 , 1700 and a larger area from 800 – 1160 cm^{-1} (SI, Figure S6). Loadings plots for PC3 (SI, Figure S7) have a significant region from 1690 – 1750 cm^{-1} , corresponding to the carbonyl groups from esters and to 4-en, 3-one steroids, illustrating that the third PC is responsible for differentiation based on API contents.

Further analyses of the subgroups formed by the OR and TP categories (Figure 4B) showed that OR ampoules were subgrouped based on their “age”. One of the subgroups (PC3 values around 2) was comprised of the new ampoules, purchased in 2014, and the other (PC3 values around -1 to 0) of ampoules seized by the BFP in 2009–2010. The difference in the spectral profile may be due to some variation in the formulation or in the manufacturing process, or even due to some small changes

on the FTIR performance, since analysis were conducted within a five-year period. However, no clear explanation could be found for the two subgroups in the TP group. They might reflect two different illegal manufacturers, poor manufacturing practices inherent to counterfeit products, or differences in the API concentration. Since no quantitative analyses were performed, these hypotheses could not be verified.

As can be seen in the score plots (Figure 4), ampoules with benzyl benzoate (BB) or propylene glycol (TP-PR, some of the TP) are easily distinguishable from the ones containing vegetable oils or long chain esters as excipients. This classification could also be achieved by submitting the spectra to a search in the FTIR library, illustrating one great advantage of FTIR over near infrared (NIR), for which spectral libraries are not always available. As these counterfeits can be detected by FTIR, they were not included in the modeled classes for the multivariate data analysis, and the PLS-DA was trained only with the OR ampoules and those in the TP group that clustered with them in the 2D score plot (Figure 4A). The other samples were used as a second test set to evaluate the efficiency of the PLS-DA method with unmodelled counterfeits.

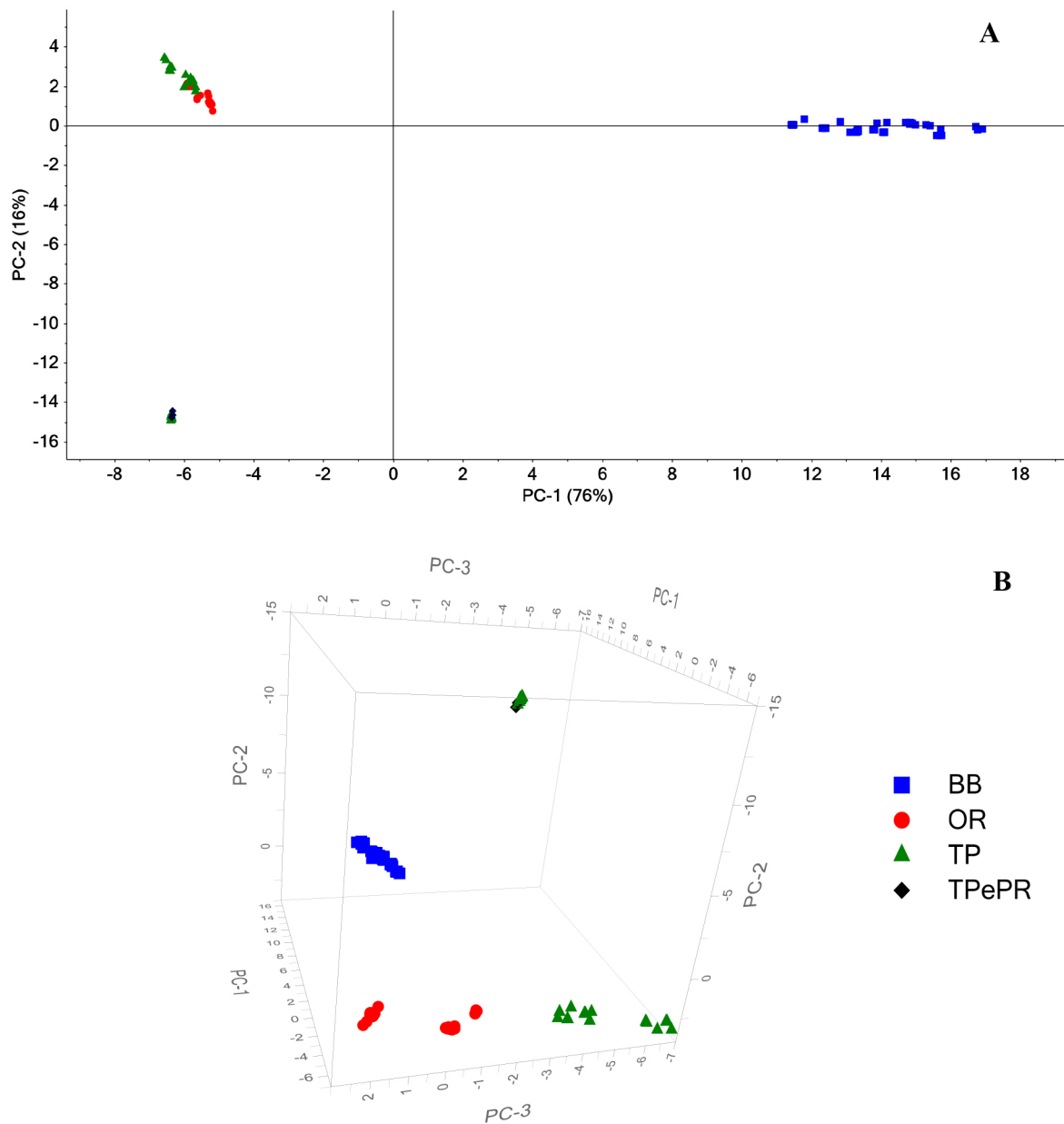


Figure 4. 2D score plot (A) and 3D score plot (B) of the 178 FTIR spectra. BB = benzyl benzoate; OR = original, TP = testosterone propionate, TPePR = testosterone propionate and prasterone.

PLS-DA

PCA is an exploratory tool to detect tendencies in a group of samples, showing which characteristics can be used for class separation,¹⁹ and it was possible to visualize all subgroups in this study using this tool (Figure 4B). However, since forensic results demand a high level of statistical certainty to be issued, and to avoid the visual/subjective interpretation of the PCA score plot, PLS-DA was used to develop a method that could be implemented as a routine analysis and yield results for which confidence limits could be estimated.

A PLS-DA model was constructed based on three latent

variables (LV) to discriminate the OR ampoules (93 spectra; Table 1) from seized TP ampoules with vegetable oils or long-chain esters (21 spectra). Two-thirds of the spectra (62 OR and 14 TP) were used as a training subset and one-third (31 OR and 7 TP) as a test subset. Training and test subsets were selected randomly, making sure that both included ampoules from the two OR and TP subgroups (Figure 4B). If replicates from a single ampoule were available, all replicates were assigned to the same subset. As the model obtained was successful in discriminating all spectra of the test subset, another model was built using half the spectra as a training set, which was also successful in discriminating the other half of the spectra. Finally, a third

model was built using one-third of the spectra as a training subset and two-thirds of the spectra as a test subset. This third model was also developed with three LV, explaining 99.6% of the total variance, and it was also successful in discriminating all spectra in the test subset.

The analysis of the Hotelling T^2 and residuals Q statistics showed that no outliers were present on the training or test subsets, since no samples presented simultaneously values of Hotelling T^2 and residuals Q above the defined limits (Figure 5A). On the other hand, all samples of the second test subset (unmodelled counterfeit samples from the BB and TP-PR groups, as well as those from the TP groups whose main excipient was propylene glycol), were considered outliers (Hotelling T^2 and residuals Q far above the threshold, Figure 5B). This result shows that the Hotelling T^2 and residuals Q can identify samples belonging to classes not included in the training set and

prevent discrimination errors for unmodelled classes. Recently, Rodionova *et al.*²⁸ argued that PLS-DA or other discrimination models cannot be used for certification models due the risk of wrongly identify a sample belonging to an unmodelled class to the target/original class. However, the analysis of the Figure 5B shows that the Hotelling T^2 and residuals Q can prevent this kind of error.

The final model showed sensitivity and specificity equal to 100%, false positive and false negative rates equal to zero and efficiency rate equal to 100%, as illustrated in Figures 6 and 7. Regression coefficients of the PLS-DA model (SI, Figure S8) showed similar behavior when compared to the loadings plot for PC3 (SI, Figure S7), indicating that the most relevant regions for discrimination were between 1770 and 1600 cm^{-1} , corresponding to the carbonyl groups of the esters and to the conjugated ketone of testosterone.

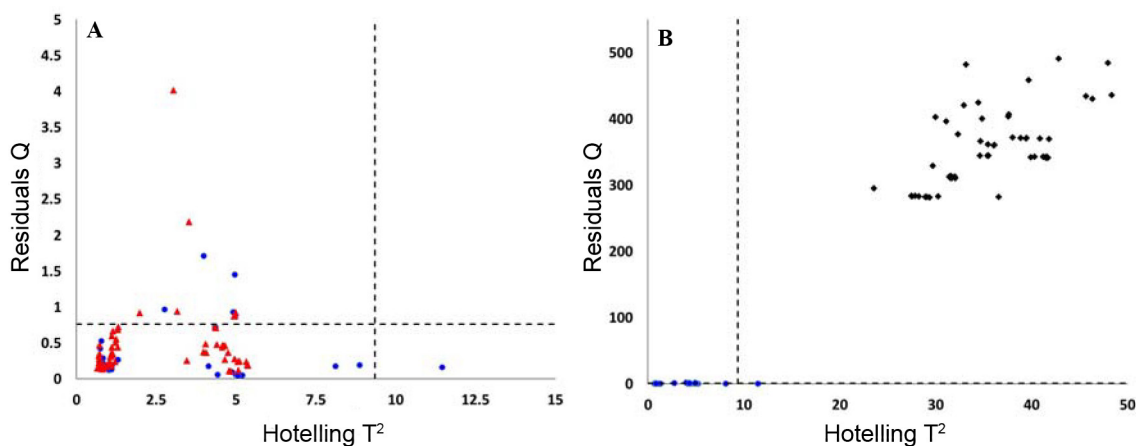


Figure 5. Dispersion plot of Hotelling T^2 versus residuals Q statistics for (A) the training subset (●) and test subset (▲); and (B) training subset (●) and unmodelled counterfeits test subset (◆). Dashed lines indicate limit values for Hotelling T^2 and residuals Q with 95% confidence for 3 PLS factors.

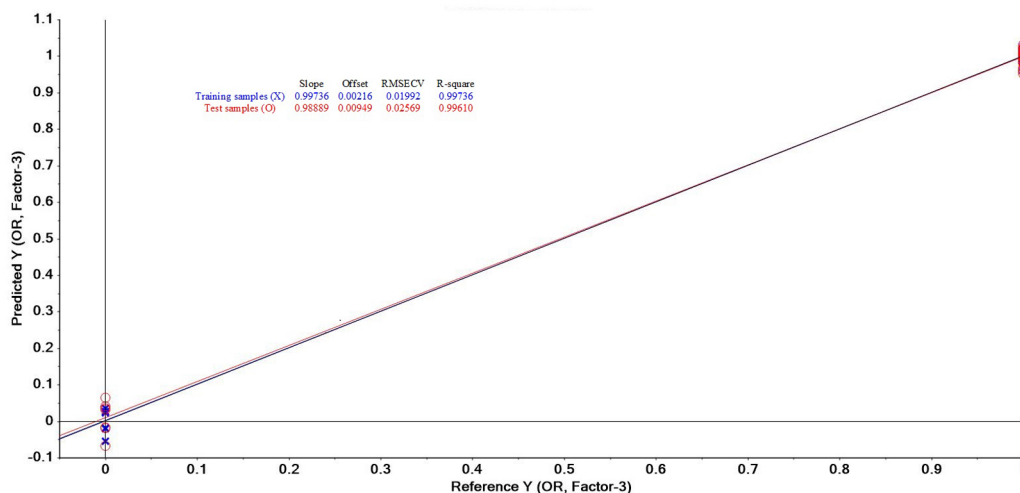


Figure 6. Class prediction plot of the PLS-DA model built to discriminate original (OR) and counterfeit (TP) ampoules. Estimated values for the training and test samples are shown in blue (×) and red (○), respectively. TP ampoules have values between -0.07 and 0.06 , whereas OR ampoules have values between 0.95 and 1.03 .

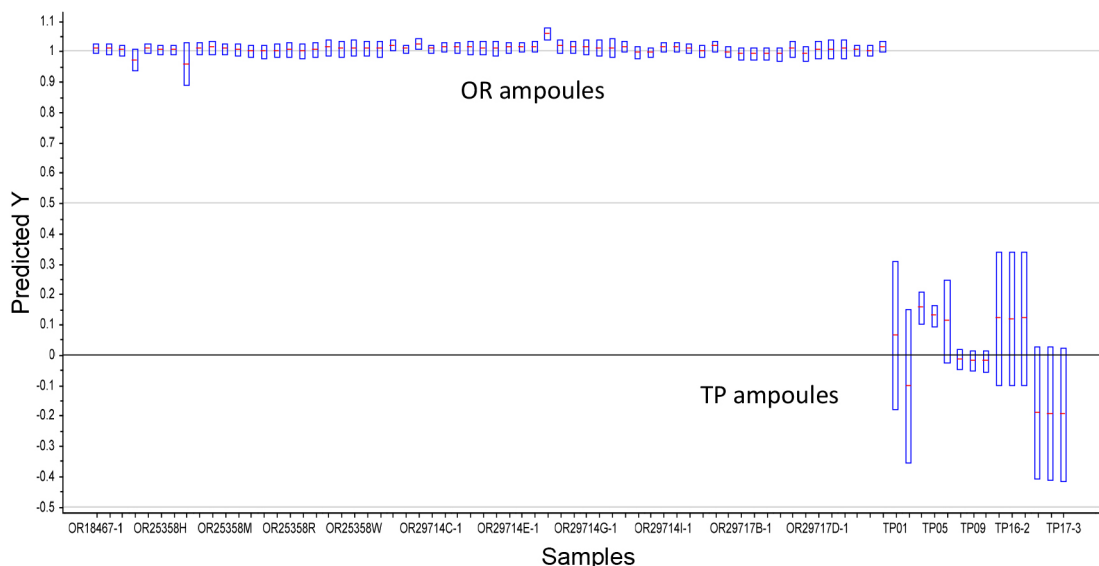


Figure 7. Class values of the test subset for original (OR) and counterfeit (TP) ampoules. The discrimination threshold was defined as 0.5.

Values of RMSECV obtained for training and test sets were low and similar (0.020 and 0.026, respectively; Figure 6), indicating no overfitting of the model and a high discrimination capability. The variation of the estimated values for classes 0 (TP) and 1 (OR) in the training samples were -0.07 to 0.06 , and 0.95 to 1.03 , respectively (Figure 6), which indicate a high discrimination power between the classes. It is important to note that in PLS-DA, the discrimination threshold is more commonly determined by a Bayesian approach, which considers the distributions of the estimated class values of the training samples.²³ For this particular application, as the variations for each class were extremely close, the Bayesian approach would result in a value very close to 0.5, therefore this value was adopted and the application of the Bayesian approach was not necessary.

Class values and confidence limits obtained for the test set were lower than the defined threshold (Figure 7). Values obtained for OR test samples ranged from 0.95 to 1.06 (maximum error 0.071) whereas values for TP test samples ranged from -0.20 to 0.15 (maximum error 0.218). There were no misclassifications and no unclassified samples (100% efficiency rate), confirming the applicability of the method in differentiating original from counterfeit samples of Durateston®.

A 100% efficiency rate was also achieved by Fernandes *et al.*¹⁶ for discriminating original and counterfeit glibenclamide tablets by NIR and fluorescence spectroscopy along with SIMCA, PLS-DA and unfolded PLS-DA. Sacré *et al.*¹³ achieved similar result by combining FTIR and NIR or FTIR and Raman spectroscopy associated with PLS analysis for Viagra-like

and Cialis-like samples, respectively. For the same products, Custers *et al.*¹⁹ achieved a 90.5% performance when discriminating genuine and counterfeit samples using FTIR and SIMCA.

Conclusions

Anabolic steroids are a frequent target for medicine counterfeiting, and Durateston® is the most frequent steroid medicine counterfeited in Brazil. Crude counterfeits, when the main excipient is drastically altered, could be detected by a simple FTIR analysis and a library search. However, FTIR followed by PLS-DA has proven to be a suitable tool for discriminating original samples from more elaborate counterfeits. The proposed PLS-DA method successfully classified all samples of the test subset, with a 100% efficiency rate. It is a robust, cheaper and far less time-consuming alternative approach to the routine GC-MS analysis of suspect Durateston® samples, and can be easily implemented in all forensic laboratories from the BFP to standardize and improve Durateston® analysis.

Supplementary Information

Supplementary data are available free of charge at <http://jbc.ssbq.org.br> as PDF file.

Acknowledgments

The authors would like to thank the National Institute of Criminalistics for allowing the execution of this work.

References

1. <http://www.who.int/medicines/regulation/ssffc/definitions/en/>, accessed in September 2016.
2. <http://www.who.int/mediacentre/factsheets/fs275/en/>, accessed in September 2016.
3. Dégardin, K.; Roggo, Y.; Margot, P.; *J. Pharm. Biomed. Anal.* **2014**, *87*, 167.
4. <https://www.gphf.org/images/downloads/impactbrochure.pdf>, accessed in September 2016.
5. Fernandez, F. M.; Green, M. D.; Newton, P. N.; *Ind. Eng. Chem. Res.* **2008**, *47*, 585.
6. Ames, J.; Souza, D. Z.; *Rev. Saúde Pública* **2012**, *46*(1), 154.
7. Neves, D. B. J.; Marcheti, R. G. A.; Caldas, E. D.; *Forensic Sci. Int.* **2013**, *228*, e81.
8. Pellegrini, M.; Rotolo, M. C.; Giovannandrea, R. D.; Pacifici, R.; Pichini, S.; *Ann. Toxicol. Anal.* **2012**, *24*(2), 67.
9. Thevis, M.; Schrader, Y.; Thomas, A.; Sigmund, G.; Geyer, H.; Schänzer, W.; *J. Anal. Toxicol.* **2008**, *32*, 232.
10. Musshoff, F.; Daldrup, T.; Ritsch, M.; *J. Forensic Sci.* **1997**, *42*(6), 1119.
11. Coopman, V.; Cordonnier, J.; *Ann. Toxicol. Anal.* **2012**, *24*(2), 73.
12. Ritsch, M.; Musshoff, F.; *Sportverletz Sportsch.* **2000**, *14*(1), 1.
13. Sacré, P.-Y.; Deconinck, E.; De Beer, T.; Courselle, P.; Vancauwenbergh, R.; Chiap, P.; Crommen, J.; De Beer, J. O.; *J. Pharm. Biomed. Anal.* **2012**, *53*, 445.
14. Kwok, K.; Taylor, L. S.; *J. Pharm. Biomed. Anal.* **2012**, *66*, 126.
15. Ortiz, R. S.; Mariotti, K. C.; Fank, B.; Limberger, R. P.; Anzanello, M. J.; Mayorga, P.; *Forensic Sci. Int.* **2013**, *226*, 282.
16. Fernandes, R. S.; Costa, F. S. L.; Valderrama, P.; Março, P. H.; Lima, K. M. G.; *J. Pharm. Biomed. Anal.* **2012**, *66*, 85.
17. Storme-Paris, I.; Rebiere, H.; Matoga, M.; Ciaved, C.; Bonnet, P.-A.; Tissier, M. H.; Chaminade, P.; *Anal. Chim. Acta* **2010**, *658*, 163.
18. De Peinder, P.; Vredendregt, M. J.; Visser, T.; de Kaste, D.; *J. Pharm. Biomed. Anal.* **2008**, *47*, 688.
19. Custers, D.; Cauwenbergh, T.; Bothy, J. L.; Courselle, P.; De Beer, J. O.; Apers, S.; Deconinck, E.; *J. Pharm. Biomed. Anal.* **2015**, *112*, 181.
20. Rebiere, H.; Ghyselinck, C.; Lempereur, L.; Brenier, C.; *Drug Test. Anal.* **2016**, *8*, 370.
21. Rajalahti, T.; Kvalheim, O. M.; *Int. J. Pharm.* **2011**, *417*, 280.
22. da Silva, V. A. G.; Talhavini, M.; Zacca, J. J.; Trindade, B. R.; Braga, J. W. B.; *J. Braz. Chem. Soc.* **2014**, *25*, 1552.
23. Ferreira, M. M. C.; *Quimiometria - Conceitos, Métodos e Aplicações*, 1ª ed.; Editora Unicamp: Campinas, Brazil, 2015.
24. Botelho, B. G.; Reis, N.; Oliveira, L. S.; Sena, M. M.; *Food Chem.* **2015**, *181*, 31.
25. Kasal, A.; Budesinsky, M.; Griffiths, W. J. In *Steroid Analysis*, 2nd ed.; Makin, H. L. J.; Gower, D. B., eds.; Springer Dordrecht Heidelberg: London, England, 2010, ch. 2.
26. Coates, J. In *Encyclopedia of Analytical Chemistry*; Meyers, R. A., ed.; John Wiley & Sons Ltd.: Chichester, UK, 2006, p. 10815.
27. Pretsch, E.; Bühlmann, P.; Badertscher, M.; *Structure Determination of Organic Compounds*, 4th ed.; Springer-Verlag: Berlin, Germany, 2009.
28. Rodionova, O. Y.; Titova, A. V.; Pomerantsev, A. L.; *Trends Anal. Chem.* **2016**, *78*, 17.

Submitted: August 23, 2016

Published online: November 4, 2016